Nuclear Technology

ISSN: 0029-5450 (Print) 1943-7471 (Online) Journal homepage: https://www.tandfonline.com/loi/unct20

Comprehensive Analysis and Evaluation of Fukushima Daiichi Nuclear Power Station Unit 2

Takuya Yamashita, Ikken Sato, Takeshi Honda, Kenichiro Nozaki, Hiroyuki Suzuki, Marco Pellegrini, Takeshi Sakai & Shinya Mizokami

To cite this article: Takuya Yamashita, Ikken Sato, Takeshi Honda, Kenichiro Nozaki, Hiroyuki Suzuki, Marco Pellegrini, Takeshi Sakai & Shinya Mizokami (2020): Comprehensive Analysis and Evaluation of Fukushima Daiichi Nuclear Power Station Unit 2, Nuclear Technology, DOI: 10.1080/00295450.2019.1704581

To link to this article: https://doi.org/10.1080/00295450.2019.1704581

NUCLEAR TECHNOLOGY

DOI: https://doi.org/10.1080/00295450.2019.1704581

Comprehensive Analysis and Evaluation of Fukushima Daiichi Nuclear Power Station Unit 2

Takuya Yamashita,[a,b]* Ikken Sato,[a,b] Takeshi Honda,[c] Kenichiro Nozaki,[c] Hiroyuki Suzuki,[d] Marco Pellegrini,[d,e] Takeshi Sakai,[b,f] and Shinya Mizokami[a,c]

[a]*Japan Atomic Energy Agency, Ibaraki, Japan*
[b]*International Research Institute for Nuclear Decommissioning, Tokyo, Japan*
[c]*Tokyo Electric Power Company Holdings, Inc., Tokyo, Japan*
[d]*Institute of Applied Energy, Tokyo, Japan*
[e]*The University of Tokyo, Tokyo, Japan*
[f]*Hitachi-GE Nuclear Energy, Ltd., Ibaraki, Japan*

Received October 7, 2019
Accepted for Publication December 10, 2019

Abstract — *Estimation and understanding of the state of the fuel debris and fission products inside the plant comprise an essential step in the decommissioning of Tokyo Electric Power Company Holdings' Fukushima Daiichi nuclear power station (1F). However, because of the plant's high-radiation environment, direct observation of the plant interior is difficult. Therefore, in order to understand the plant's interior conditions, comprehensive analysis and evaluation based on various measurement data from the plant, analysis of plant data during the accident progression phase, and information obtained from computer simulations for this phase are necessary. These evaluations can be used to estimate the conditions of the interior of the reactor pressure vessel (RPV) and the primary containment vessel (PCV). This paper addresses 1F Unit 2 as the subject to produce an estimated map of the fuel debris distribution from data obtained about the RPV and PCV based on comprehensive evaluation of various measurement data and information obtained from the accident progression analysis, which were released to the public in June 2018.*

Keywords — *Fukushima Daiichi, severe accident, decommissioning.*

Note — *Some figures may be in color only in the electronic version.*

I. INTRODUCTION

The task of decommissioning Tokyo Electric Power Company Holdings' (TEPCO's) Fukushima Daiichi nuclear power station (1F), which suffered a severe accident (SA) on March 2011, is underway. The estimation and comprehension of the state of the fuel debris and fission products (FPs) inside the nuclear reactor are essential for the decommissioning of 1F. However, the conditions inside the reactor pressure vessel (RPV) and the primary containment vessel (PCV) after the accident are extremely difficult to understand for the following reasons. Direct observation of the plant interior is difficult because of the high-radiation environment. Units 1, 2, and 3 of 1F lost their cooling functions and direct-current electric power supply during the tsunami, so measurements from the on-board meters are difficult to collect. Thus, information collected during the accident progression itself is in short supply. Existing research at 1F has been mainly conducted for the decommissioning of 1F. Thus, some exceptions like

*E-mail: yamashita.takuya38@jaea.go.jp

information of dose rate distribution are not systematically managed; therefore, the information is scattered among different sections. Moreover, the SA code used to analyze the behavior of the entire plant during a SA is largely uncertain because the explanation of each phenomenon is incomplete.

For these reasons, various information from inspections of the accident site should be collected to describe the main sections of each unit. This information should be combined with the analysis of data recorded during and after the accident, knowledge obtained from simulated tests, and accident progression analysis. These varied data sources should be compared to verify their consistency, and a comprehensive evaluation is required to accurately estimate the conditions inside the RPV and PCV. The results of the comprehensive evaluation were published in July 2017 as the first edition by TEPCO (Ref. 1). These charts are regularly updated to reflect the latest information in the project of Decommissioning and Contaminated Water Management (Upgrading Level of Grasping State Inside Reactor).[2]

This study aims to provide information that will aid in the decommissioning of 1F. Hence, based on the accident progression analysis for 1F Unit 2, which was released to the public in June 2018, an estimated map of the fuel debris distribution in the RPV and PCV was prepared from the comprehensive evaluation of various data collected from the accident site. The basis for the estimation of the fuel debris distribution in the RPV and PCV is explained therein.

II. CHARACTERISTICS OF ACCIDENT PROGRESSION AT UNIT 2

Figure 1 (Ref. 1) shows the relationship between the decay heat of Unit 2 and the heat generated via the zirconium-water reaction. At Unit 2, the reactor core isolation cooling (RCIC) system continued to function for approximately 3 days after the accident, which continued the cooldown of the fuel until the decay heat began to decrease. After the failure of the RCIC system, the water level decreased because of the decay heat. The RPV was rapidly decompressed by manually opening the main safety relief valve (SRV) when the water level reached the top of the fuel, and this caused decompression boiling and a further decrease of water level, which is assumed to have eventually exposed the fuel. By the time the fire engines started to inject water into the RPV, the fuel was already exposed. This exposure suggests that the zirconium-water reaction began when water vapor came into contact with the heated fuel, causing the fuel to melt.

The extent of the damage to the fuel in Unit 2 is highly dependent on the extent to which the water injection from fire engines reached the interior of the RPV.

III. INFORMATION AGGREGATION

Figure 2 (Ref. 2) and Table I (Refs. 3 through 47) show the collected information that contributes to the estimation of the fuel debris distribution in the RPV and PCV of Unit 2. The information shown in Table I (Refs. 3

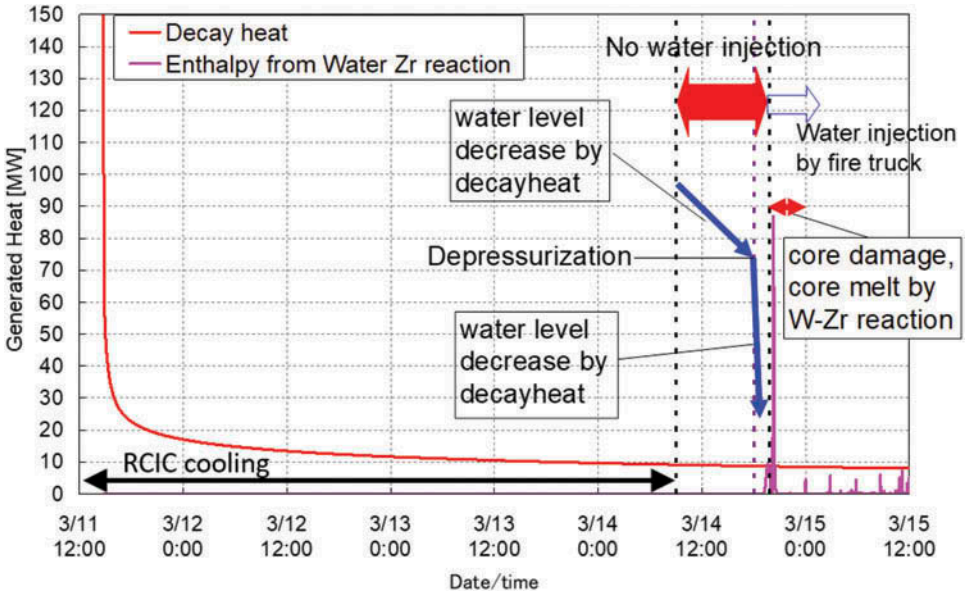

Fig. 1. Relationship between the decay heat of Unit 2 and the heat generated via zirconium-water reaction.[1]

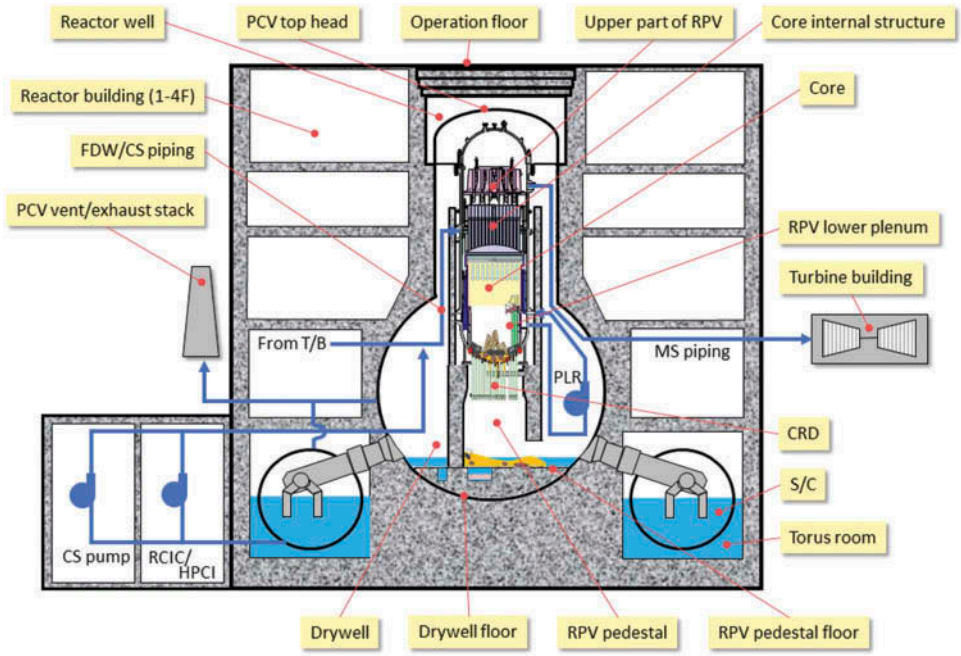

Fig. 2. Unit 2 information aggregation.[2]

through 47) is categorized based on whether it involves direct or estimated measurements, analysis from the SA code, or a qualitative estimation.

IV. ESTIMATION OF THE CONDITIONS OF RPV AND PCV

The estimated map of fuel debris distribution in the RPV and PCV, shown in Fig. 3 (Ref. 2), was prepared based on a comprehensive evaluation of the aggregated information (Fig. 2 and Table I), all of which was deemed relevant to the state of the RPV, PCV, and reactor building of each unit. The remainder of this section provides explanations of the basis for the estimation of each part of the main sections in the map of fuel debris distribution shown in Fig. 3 (Ref. 2).

IV.A. Reactor Core

IV.A.1. Estimation 1 (Significant Fuel Melting During the Second Pressure Peak)

Even though the RPV at Unit 2 was successfully decompressed at 18:00 on March 14, 2011, with the forced opening of the SRV, three increases in the RPV pressure occurred between the evening and the following morning [Fig. 4 (Refs. 1 and 48)]. According to the records, this behavior is considered to have come along with the opening/closing of the SRV (pressure increase = SRV closed; pressure decrease = SRV opened). However, this does not mean that the opening/closing of the SRV was verified. The increase in the containment pressure is likely caused by the generation of a large amount of hydrogen, and this increase in pressure likely made a significant contribution to the accident progression at Unit 2. This is because the generation of hydrogen that accompanies the zirconium-water reaction is exothermic; therefore, the generation of a large amount of hydrogen generates a large amount of energy, which, in turn, indicates the extent of melted fuel. To better understand this pressure behavior in the nuclear reactor, and find a realistic amount of generated water vapor and hydrogen gas [Fig. 5 (Refs. 1 and 48)], the actual measurements of the RPV and drywell (D/W) pressure were reproduced using the thermal-hydraulic code Generation of Thermal-Hydraulic Information for Containments (GOTHIC). For this reproduction of the actual measurement of pressure and realistic generation amount of vapor and hydrogen, the amount generated in Fig. 6 (Refs. 1 and 48) was assumed. These results show that by the second peak, almost all the zirconium inside the reactor could have reacted and the amount of generated hydrogen became particularly conspicuous. Therefore, based on the relationship between the amount of generated hydrogen accompanying the zirconium-water reaction and energy generation, it is considered that a significant amount of the fuel could have melted during the second peak.

Therefore, the amount of generated energy was inferred to be based on the pressure increase in the PCV

TABLE I

Collected Information About Unit 2*

Core internal structure	• **The PLR system pressure increases with the FDW flow rate**.[3] *The water level outside the shroud likely increased.* • *Because of the temperature decrease accompanied by the CS water injection and increase in the water level outside the shroud when the amount of water injection increased, the shroud likely remains.* • FPs are inferred to adhere to the separator and the dryer. • Cesium may be integrated in the oxidized steel bed. • Cesium may have combined with molybdenum, boron, and silicon.
Core	• **Interior of the traversing in-core probe (TIP) piping is blocked**.[5] • **Scanning electron microscope analysis of elements blocking the TIP piping detected Zr, which is a constituent element of the fuel cladding and the reactor internal structure in addition to the constituent elements of steel, such as Fe, Cr, Ni, and Mn (**Refs . 6 and 7**). No water was found in the reactor core region**.[3] • Some debris may have solidified in the upper part of the speed limiter inside the CRGT and remains (when the CRD piping is intact). • *Results of the muon measurement indicate the possibility of fuel around the periphery of the reactor core region*.[8]
Upper part of RPV	• **Temperature of the upper part of the RPV is higher than that of the lower part of the RPV** (Ref. 8). • A large amount of FPs are present. • The chemical form of the adhered FP is not known (e.g., whether it is water soluble). • The extent of reevaporation of adhered FP is unknown.
Reactor well	• *Similar to Unit 3, there exists a high-contamination area in the gap between the highest level and the shield plug of the level below.* • *The level below and the reactor well are also highly contaminated.* • Particle-shaped FPs may be present.
PCV top head	• *The seal of the PCV top head deteriorated to make an opening for the leakage of water vapor and FPs.*
RPV lower head	• **The outer circumference of the RPV lower head suffered no extensive damage, such as the whole RPV lower head falling, attributed to the intact CRD cables**.[9] • **An opening was formed by the damage because water did not accumulate in the RPV (**Ref. 10). • **A thermometer was installed through the standby liquid control (SLC) piping**.[11] *(The temperature setting is greater than the water injection temperature, and the temperature is inferred to have increased inside the RPV because of the fuel debris.)* • The opening is located in the center and periphery of the RPV lower head. • A small amount of water has accumulated because the temperature response to changes in water injection is relatively fast.[12] • *The temperature responses of RPV and PCV to the reduction of the rate of water injection in March and April 2017 suggest the presence of fuel debris at the bottom of the RPV* (Ref. 13). • *High-density matter found in the muon measurement results is likely to be fuel debris*.[8] • **A temperature change of a few degrees Celsius was observed at the bottom part of the RPV in response to the individual water injections from the CS and FDW systems**.[14,15]
Reactor building (1–4 floor)	• **Ambient dose rate of a few to a few dozen mSv/h is inferred from April 2011 to February 2014** (Ref. 16). • **Local high radiation rates occur at the locations of penetrations**.[17,18] • **At a few mSv/h, no conspicuous contamination in the TIP room is inferred on March 3, 2014** (Ref. 19).
Operation floor	• **Maximum dose is ~880 mSv/h on June 30, 2012** (Ref. 20). • *Dose distribution in well → blow out panel direction*.[21]

(Continued)

TABLE I (Continued)

CRD	• **CRD and cables remain intact around the outer circumference of the RPV lower head.**[9,22] • **Accumulation on the CRD exchange rail was verified.**[23] • **No extensive damage to the CRD housing support was observed.**[24] • **In some sections the TIP guiding tube and local power range monitoring (LPRM) cables cannot be observed. The grating right beneath the CRD was verified to have fallen.**[24]
FDW/CS piping	• **A temperature drop was observed when the CS water injection began.**[10] • *Debris is inferred to be in the path from the CS to the lower plenum that goes through the reactor core.*
RPV lower plenum	• **Blockage in the SLC piping inside the RPV** (Ref. 25). • **A thermometer was installed through the SLC piping.**[26] *(Temperature setting of the SLC piping is greater than the water injection temperature, and the temperature is inferred to have increased inside the RPV due to the fuel debris.)* • The heat balance evaluation suggests that ~30% remains.[27]
PCV vent/exhaust stack	• **High contamination at a few to a few dozen Sv/h was verified at the exhaust stack shared by Units 1 and 2, the vent line of Unit 2, and the stand-by gas treatment system (SGTS) of Unit 2 from March 26, 2012, to March 27, 2012** (Ref. 28). • **High contamination at a few dozen mSv/h to ~1 Sv/h was verified at the lower part of the exhaust stack, and high contamination at 500 mSv/h to 2 Sv/h was verified at the joints of the SGTS piping from August 6, 2014, to October 21, 2015** (Ref. 29). • *Because the ruptured disk of Unit 2 is inferred to be undamaged, this contamination is inferred to have originated from Unit 1* (Ref. 30). • **The extent of contamination did not change from before to after the disk rupture, and it is low.**[30] Thus, the venting is inferred to have been unsuccessful.
Drywell	• **The ambient dose rate of the D/W (70 Sv/h) is high relative to other units.**[28] • **Pulverized fallen objects were found.**[31] • **The cesium concentration of the stagnant water inside the PCV is higher than that of the stagnant water in the building but has the same level as strontium and H_3 concentrations.**[32] • From the pressure and oxygen concentrations, the gas phase leakage is inferred to be relatively small. • **The maximum D/W containment atmospheric monitoring system (CAMS) was 138 Sv/h on March 15, 2011, 16:00** (Ref. 33). *From the transition of the indicated CAMS value, the maximum dose of 138 Sv/h is estimated to be attributed to fuel debris falling within the containment vessel because of the breakage of the RPV* (Ref. 34). • **High radiation at <10 Gy/h to ~80 Gy/h was verified near the CRD rail from January 26, 2017, to February 9, 2017** (Ref. 35). • **Dose between ~24 and 36 Sv/h was verified near the CRD exchange rail and the opening of the pedestal on August 12, 2013** (Ref. 9).
Drywell floor	• **Debris was not found during the internal inspection of the PCV. There was a small amount of accumulation.**[31] • **Water level was ~30 cm, equal to the lower end of the PCV vent pipe.**[36] • *As the S/C had no accumulated water, water also does not accumulate in the D/W* (Ref. 37).
RPV pedestal	• **CRD and cables remain in the outer circumference of the lower head.**[9] • **No extensive damage to the existing structure (CRD exchanger) was found.**[38] • **The water flowing into the RPV fell on the pedestal.**[39] • **The state of the damage to the grating of the platform in the pedestal was verified and was possibly due to thermal effects of the fuel debris. Adherence of accumulations at several spots was verified.**[22,35,40,41] • **Dose around 10 Gy/h or less was verified near the inner wall of the pedestal on January 30, 2017** (Ref. 35). • **No extensive damage to the inner wall of the pedestal was found.**[38,39] • **The dose rate from the height of the platform near the inner wall of the pedestal (CRD rail side) to ~2 m below the pedestal was around 7 to 8 Gy/h, the temperature was 21 °C, and no major change was observed.**[38]

(Continued)

TABLE I (Continued)

RPV pedestal floor	• **Part of the fuel assembly was verified to have fallen at the bottom of the pedestal**. *The accumulations verified around it are inferred to be fuel debris*.[38,39,42] • **Accumulation is verified to cover all of the pedestal floor**.[38,39] *It may contain fuel debris.*
Torus room	• **S/C and the torus room have almost identical water levels**.[43] • **The difference in water level is attributed to the difference between the S/C pressure and atmospheric pressure**.[44] • *The reactor building (R/B) and the turbine building (T/B) are somehow connected*.[45] • **Inspection showed the atmospheric dose to be 4.3 to 134.0 mSv/h and the underwater** • **dose to be 18.7 to 23.7 mSv/h in April, 2013** (Ref. 46). • **Cesium-134 and ^{137}Cs were detected in the collected stagnant water, on the order of 10^4 Bq/cm^3 on April 12, 2013 (**Ref. 4). • **The inspection did not verify leakage near the vent pipe**.[47]
S/C	• **S/C and the torus room have almost identical water levels**.[43] • *The opening formed by the damage is at the lower part of the S/C (inferred to be less than OP512)* (Ref. 44). • Forced decompression by the SRV was conducted at Unit 2 after the core was damaged. Thus, as observed at the S/C CAMS, a large amount of FPs had moved to the S/C. Note that the FPs captured by the pool water likely moved to the building through the opening in the lower part of the S/C.
Turbine building	• **Ambient dose rate at a few dozen μSv/h from April 2011 to February 2014 (**Ref. 16). • **High radiation in the basement from April 2011 to February 2014** (Ref. 16). • *Highly contaminated water likely flowed in from the opening at the bottom of the S/C.*

*From Refs. 3 through 47. Bold typeface: measurement results/information; italic typeface: estimation from the measurement results/observation results; regular typeface: accident analysis or qualitative estimation.

caused by the amount of generated hydrogen, and a significant amount of the fuel could have melted.

IV.A.2. Estimation 2 (Remaining Fuel in the Core Periphery: CS Data)

As shown in Fig. 7 (Refs. 1 and 49), the temperature of each section of the containment vessel decreased after the water injection from the core spray (CS) system, which began on September 14, 2011. However, during the period shown in Fig. 7 (Refs. 1 and 49), after water injection from the CS system began, the maximum rate of water injection was 7.2 m^3/h, which is dramatically less than the designed flow rate of 1141 m^3/h, implying that the sprayed water is unlikely to have spread very wide with this low flow rate. Therefore, some of the fuel likely reached the sprayed water even with the low flow rate water injection from the CS system, for instance, around the periphery of the reactor core region. However, while this information indicates the possibility that a heat source was present on the outer circumference, it cannot distinguish between heat from the fuel debris that remained on the periphery of the reactor core region and heat from fuel debris that solidified after molten fuel dropped onto the fuel support. Thus, a detailed vertical fuel debris distribution cannot be inferred from this information.

Thus, as a temperature decrease clearly occurred during water injection from the CS system, it is assumed that some fuel remained on the outer circumference of the reactor core where the low flow rate of the water injection from the CS system could reach.

IV.A.3. Estimation 3 (Remaining Fuel in the Core Periphery: Muon Data)

At Unit 2, measurements using the muon-transmission method were conducted between March and July 2016 to analyze and evaluate the position of fuel debris in the RPV. Figure 8 (Ref. 18) shows the results of the evaluation of the amount of substance inside the RPV by comparing the simulation results with muon measurements at "①" the upper part of the reactor core, "②" the lower part of the reactor core, "③" the lower part of the RPV, and "④" the bottom part of the RPV. Comparing the measurement of the lower part of the reactor core ("②") and the simulated measurement shows that the measurements are closer to the result of the simulation in cases where fuel is present as compared to cases where fuel is not present. Thus, some fuel may remain around the periphery of the reactor core region.

NOTES

G E: General estimation
AM: Actual measurement
A : Analysis
E : Experiment
EA : Estimation based on actual measurement

Est. 1 (GE, A): the amount of generated energy was inferred to be based on the pressure increase in the PCV caused by the amount of generated hydrogen, and the significant amount of the fuel could have melted.
Est. 2 (AM): as a temperature decrease clearly occurred during water injection from the CS system, some fuel remained on the outer circumference of the reactor core where the low flow rate of the water injection from the CS system could reach.
Est. 3 (AM): the muon measurements imply that fuel or fuel debris may have reached the periphery of the reactor core region.
Est. 4 (GE): remaining fuel rods are likely to be found only around the periphery of the reactor core region.
Est. 5 (GE): the oxide debris was likely generated by the solidification of the melted fuel.

Est. 6 (AM): the entry pressure of the PLR system increased with the FDW flow rate, some water may have accumulated outside the shroud.
Est. 7 (AM): no extensive damage to the shroud is estimated to have occurred, as inferred from the decrease in temperature caused by the CS water injection and the increase in the water level outside the shroud.

Est. 13 (EA): the upper tie plate has fallen on the outer circumference of the pedestal, the openings formed by the damage probably exist around the outer circumference of the RPV.
Est. 14 (AM): there is a hole at least large enough for the upper tie plate to fall through.
Est. 15 (EA): judging from the debris accumulated at the bottom of the RPV, parts of the CRGT and CRD of the outer circumference melted and/or collapsed.

Est. 11 (AM): the muon measurements verified the existence of a trace of high-density matter that is probably fuel debris at the bottom of the RPV. The fuel that dropped to the lower plenum remained at the bottom of RPV.

Est. 12 (EA): the holes in the RPV are focused around its center and are not very large. As water drops were falling on the entire surface of the pedestal floor, even though some parts had more water drops than other parts, several small openings may have been formed by the damage around the control rod drive (CRD) housing at the bottom of the RPV.
Est. 16 (GE): some of the debris that fell out of the hole is adhered on the CRD.

Est. 21 (AM): the accumulation near the upper tie plate, which fell on the pedestal floor, is fuel debris that fell through the same hole on the RPV as the upper tie plate.

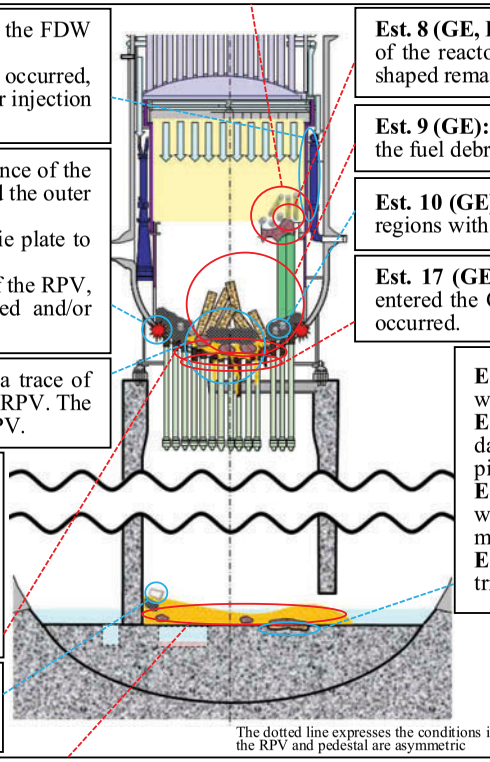

Est. 8 (GE, E, A): as the temperature increase of the fuel around the periphery of the reactor core region may not have been very high, fuel-rod or pellet-shaped remains may be found around the periphery of the reactor core region.

Est. 9 (GE): the CRGT likely remained unmelting when the heat transfer from the fuel debris was low.

Est. 10 (GE): particle or pellet-shaped fuel debris may have accumulated in regions with the stagnant flow.

Est. 17 (GE, E): a small amount of fuel debris or melted metal may have entered the CRD housing after the damage to the CRGT and CRD housing occurred.

Est. 23 (GE): the fuel debris that resulted in the MCCI is mixed in with the concrete.
Est. 24 (AM): the MCCI was limited as there was no tendency of damaged to the PCV shell (no leakage from the sand cushion drain pipe).
Est. 25 (GE, AM): the MCCI was limited because the pedestal walls, the cable tray, and the pillar of the CRD exchange mechanism did not melt.
Est. 26 (EA, A): some of the fuel debris solidified without triggering significant MCCI.

LEGEND

- Remaining fuel rods
- Oxide debris (porous)
- Granular debris
- Metal mixed debris
- Concrete mixed debris
- Sound CRGT
- Damaged CRGT
- Sound CRD
- CRD (debris inside)
- Sound shroud
- Pellets
- RPV damaged point
- Upper tie plate
- Sediment (Unknown material)

Est. 18 (GE): particle-shaped debris was formed where there is accumulated water on the PCV floor.
Est. 19 (GE): there is a possibility that when there is particle-shaped debris, it accumulates on stagnant parts.
Est. 20 (AM): accumulation containing fuel debris spreads all over the bottom of the pedestal.
Est. 22 (EA): the fuel debris on the pedestal floor has relatively low dose and decay heat and may contain large amounts of metal because no changes in dose or temperature were detected between the pedestal floor and the platform and no conspicuous damage was observed to the lower structure of the pedestal.

Fig. 3. Estimated distribution of fuel debris in Unit 2 (Ref. 2).

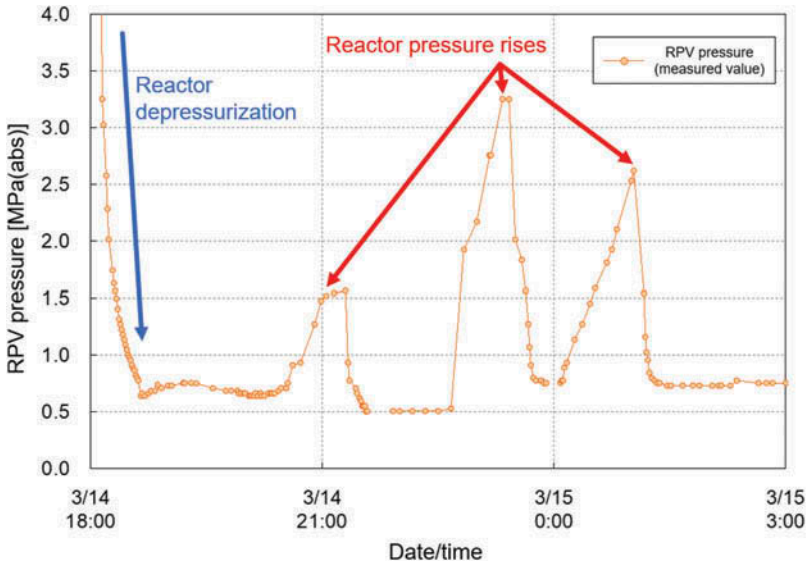

Fig. 4. The RPV pressure behavior after manually opening the main SRV (Refs. 1 and 48).

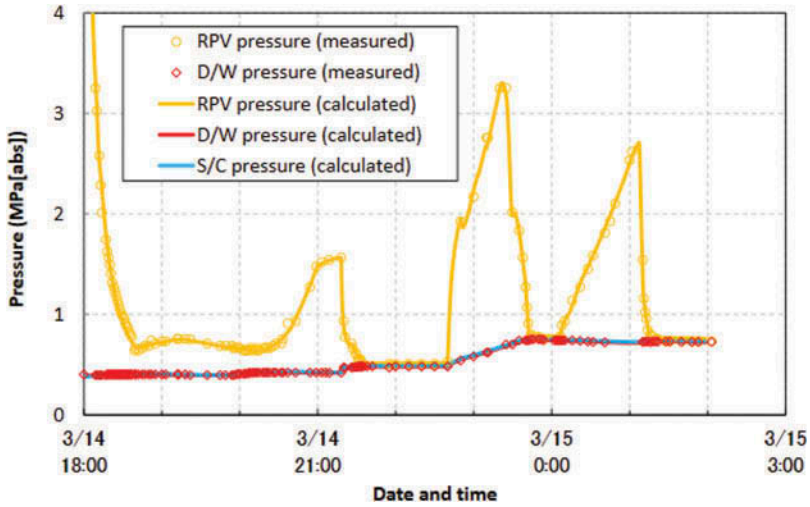

Fig. 5. Comparison of measurements of RPV/PCV pressure with the result of the GOTHIC analysis.[1,48]

Therefore, the muon measurements imply that fuel or fuel debris may have reached the periphery of the reactor core region.

IV.A.4. Estimation 4 (Remaining Fuel Rods)

The general estimation implies that the temperature of the reactor core increased from the center outward; therefore, the melting of the fuel follows the same pattern. Thus, even if some of the fuel rods remain, they are likely to be concentrated around the outer circumference.

Therefore, the remaining fuel rods are likely to be found only around the periphery of the reactor core region.

IV.A.5. Estimation 5 (Oxide Debris)

The general estimation implies that debris generated by the solidification of melted fuel can be found around the periphery of the reactor core region. The fuel that melted during the accident is assumed to have fused with similarly melted cladding and structural materials. Moreover, zirconium and iron, which are components of cladding and structural materials, respectively, are very likely to have oxidized because of the vapor-metal reaction. Thus, the main components of the debris are likely to be uranium oxide, zirconium oxide, and iron oxide from the fuel, cladding, and reactor core internal structure, respectively. Furthermore, as the phase separation of the melted mixture occurs during solidification, we infer that the oxide debris includes several phases.

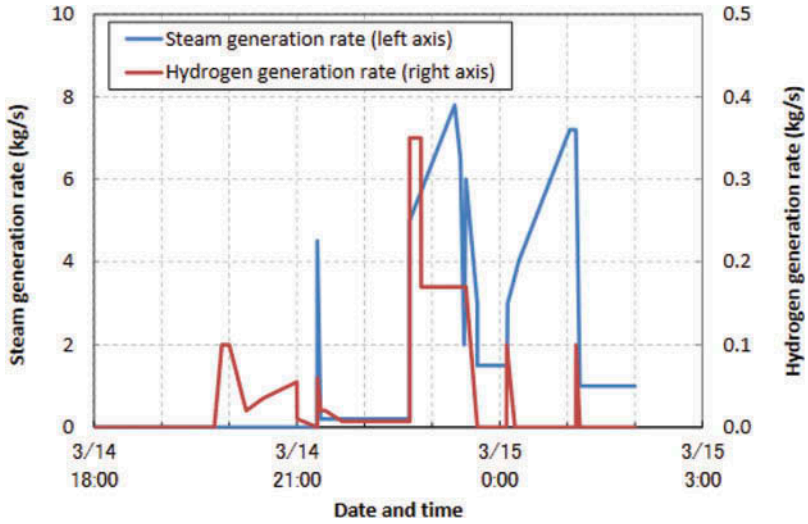

Fig. 6. Setting of the amount of generated vapor and hydrogen by the GOTHIC analysis.[1,48]

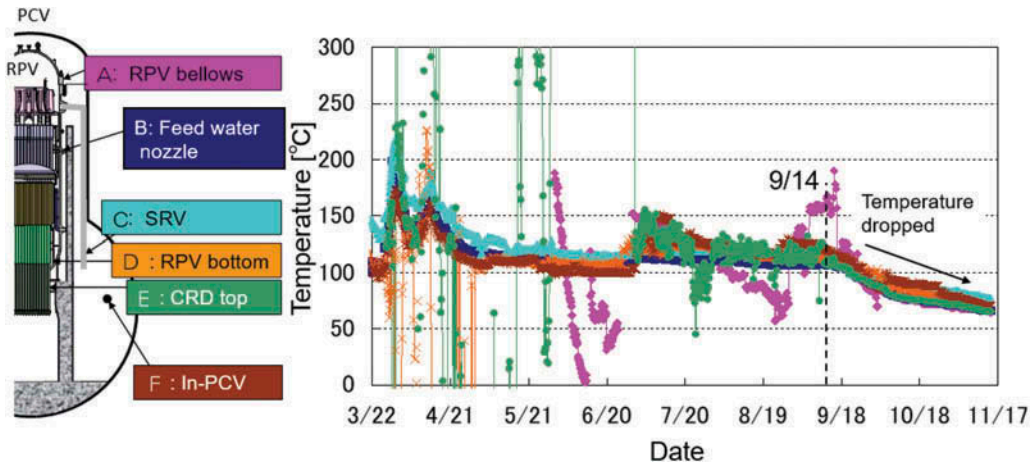

Fig. 7. Temperature of each part of the PCV in 2011 (Refs. 1 and 49).

Thus, the oxide debris was likely generated by the solidification of the melted fuel.

IV.B. Shroud

IV.B.1. Estimation 6 (Shroud Integrity: Water Injection from the FDW System)

Figure 9 (Refs. 1 and 50) shows the relationship between the amount of the water injection from the feedwater (FDW) system and the annulus water level estimated from the entry pressure of the primary loop recirculation (PLR), as recorded between December 2011 and February 2012. As the amount of water injection from the FDW system changed, the water outside the shroud increased. This relationship suggests the following two possibilities. First, the damage to the shroud may have been small so that water accumulated outside the shroud. Second, as the amount of water injection from the FDW system increased, the water level in the RPV may have increased even though the shroud was damaged.

Figure 10 shows a similar relationship between the amount of water injection from the FDW system and the annulus water level estimated from the entry pressure of the PLR as recorded between February 2013 and March 2013. During the period shown in Fig. 10, there were times when the amount of water injection from the FDW system was turned to zero without changing the total amount of water injection amount by combining the amount of water injection from the FDW system and that from the CS system twice. The annulus water level, estimated from the entry pressure of the PLR system, decreased at these two moments. This behavior is likely caused by a certain amount of water accumulated outside the shroud. Therefore, the

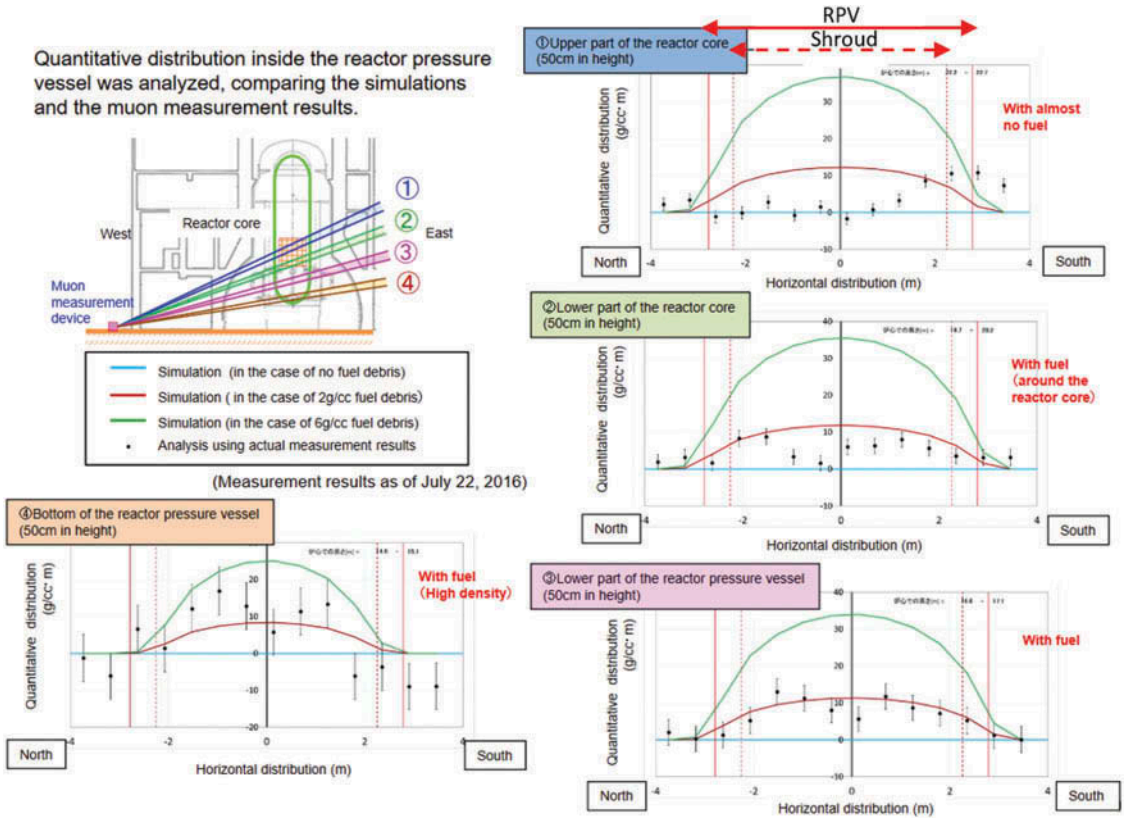

Fig. 8. Comparison of muon measurement results and simulation results.[18]

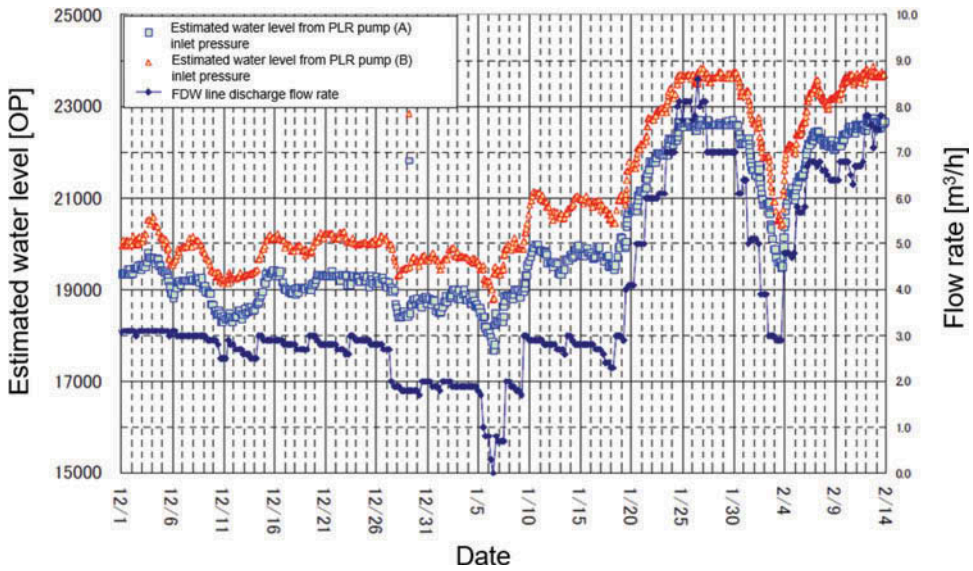

Fig. 9. Relationship between the amount of water injection from the FDW system and the annulus water level estimated from the entry pressure of the PLR system from December 2011 to February 2012 (Refs. 1 and 50).

first possibility is more likely, and it is unlikely that the shroud was extensively damaged.

Therefore, because the entry pressure of the PLR system increased with the FDW flow rate, some water may have accumulated outside the shroud.

IV.B.2. Estimation 7 (Shroud Integrity: Water Injection from the CS System)

As shown in Fig. 7 (Refs. 1 and 49), the temperature of each part of the containment vessel uniformly

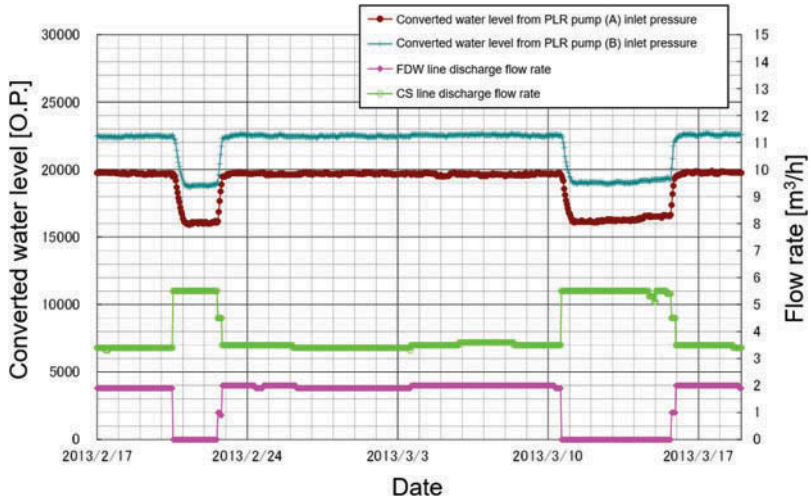

Fig. 10. Relationship between the amount of water injection from the FDW system and the annulus water level estimated from the entry pressure of the PLR system from February 2013 to March 2013 (Ref. 1).

decreased following the water injection from the CS system, which began on September 14, 2011. Note that the flow rate of water injection from the FDW system was approximately the same before and after the CS system was engaged. Moreover, based on this fact, one can infer that heat sources were located such that they could be cooled down by the water injection from the CS system, and it is unlikely that the heat sources had moved outside the shroud because of damage to the shroud. Therefore, the shroud may not be extensively damaged. Note that the integrity of the shroud support was likely affected by the height of fuel debris accumulated at the bottom of the pressure vessel. At Unit 2, approximately 10 m^3 of debris accumulated from the bottom of the pressure vessel to the lower part of the shroud support, excluding the volume of the control rod guide tube (CRGT). Considering the amounts of fuel in the reactor core and the structure at the lower part of the RPV, the accumulation of fuel at the bottom of the RPV may have reached the lower part of the shroud support. Therefore, while the shroud support may be damaged by the fuel debris, not enough information and knowledge are available to make an inference. Note that as the state of the fuel debris while moving to the bottom of the RPV differed from unit to unit owing to the difference in the accident progression, it is possible that the state of the shroud support also differed from unit to unit.

Thus, no extensive damage to the shroud is estimated to have occurred, as inferred from the decrease in temperature caused by the CS water injection and the increase in the water level outside the shroud.

IV.B.3. Estimation 8 (Remaining Fuel Rods: Estimation from Shroud Integrity)

As discussed in Sec. IV.B.1, the shroud of Unit 2 was not extensively damaged, implying that the temperature increase around the periphery of the reactor core region may not have been very high. Moreover, the results of the boiling water reactor (BWR) core degradation behavior confirmation test using a simulated duel assembly[2,51–53] show that in areas where radiative heat transfer is high, such as the periphery of the reactor core region, high temperature is not maintained. Thus, the fuel may not have completely melted and can be shaped like of columns or pellets at the bottom of the RPV.

Therefore, as the temperature increase of the fuel around the periphery of the reactor core region may not have been very high, fuel rod or pellet-shaped remains may be found around the periphery of the reactor core region.

IV.C. Lower and Bottom Parts of the RPV

IV.C.1. Estimation 9 (Condition of CRGT)

While the general estimation indicates that the temperature of the CRGT near the lower plenum of the RPV was high, particularly along the path of the fuel coming down from the reactor core, some of the CRGT may have remained unmelted in cases where the heat transfer from the fuel debris was low.

Therefore, the CRGT likely remained unmelted when the heat transfer from the fuel debris was low.

IV.C.2. Estimation 10 (Particulate Fuel Debris in Stagnant Locations)

The general estimation infers that as the structure of the lower plenum of the RPV of the BWR is complex, some parts of the fuel debris may have accumulated at locations with little flow of gas and liquid (stagnant locations) when they were in particle form, or they may have dropped to the lower plenum when still in their pellet shape.

Therefore, it is inferred that particle- or pellet-shaped fuel debris may have accumulated in regions with stagnant flow.

IV.C.3. Estimation 11 (Fuel in the Lower Head: Muon Data)

As shown in Fig. 11 (Ref. 18), the results of muon measurement conducted between March and July 2016 verified the existence of a shadow of a high-density matter that is inferred to be fuel debris at the bottom of the RPV. Thus, the fuel debris that dropped to the lower plenum probably remained at the bottom of the RPV.

Thus, the muon measurements verified the existence of a trace of high-density matter that is probably fuel debris at the bottom of the RPV. It is inferred that the fuel that dropped to the lower plenum remained at the bottom of the RPV.

IV.C.4. Estimation 12 (Multiple Failure Sites in the RPV Boundary)

As shown in Fig. 12 (Ref. 30), a research device entered from the X-53 penetration zone in August 2013 to study the exchange rail of the control rod drive mechanism (CRDM) and the area near the opening of the pedestal. A U-shaped cable appears in the photograph captured from the point indicated by "(3)" in Fig. 12 (Ref. 30), while the device was facing the inside of the pedestal. Next, Fig. 13 (Ref. 30) shows the state of the interior of the pedestal of Unit 5. Figure 13(a) was captured from the same angle as the photograph shown in Fig. 12 (Ref. 30), Fig. 13(b) shows a view from below, and the U-shaped cable resembles the one observed in Unit 2.

From the images captured in January 2017 during the inspection of the PCV interior using the guide pipe [Fig. 14 (Ref. 40) and Fig. 15 (Ref. 40)], it can be observed that the grating is about to fall along with the accumulated debris at a location closer to the center than the inner circumference of the pedestal but not at the center itself. Moreover, on observation of the upper part, because the coating of the cables maintains its shape, some fuel debris of relatively low temperatures may have fallen on this spot. Furthermore, water drops are seen falling on the entire surface of the pedestal floor in the video obtained during the internal inspection of the

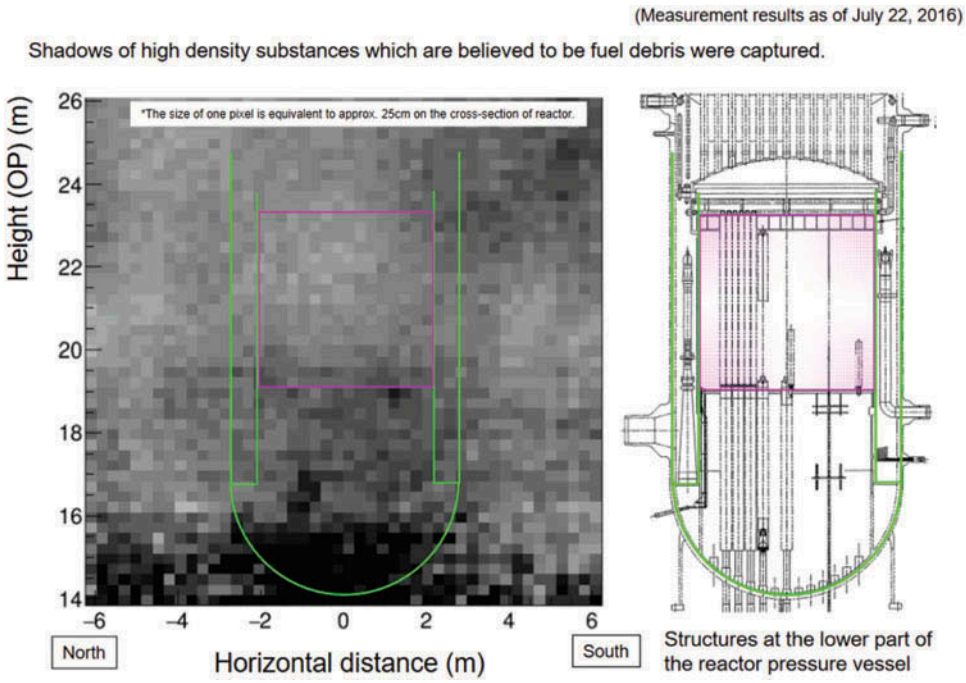

Fig. 11. Muon measurement results.[18]

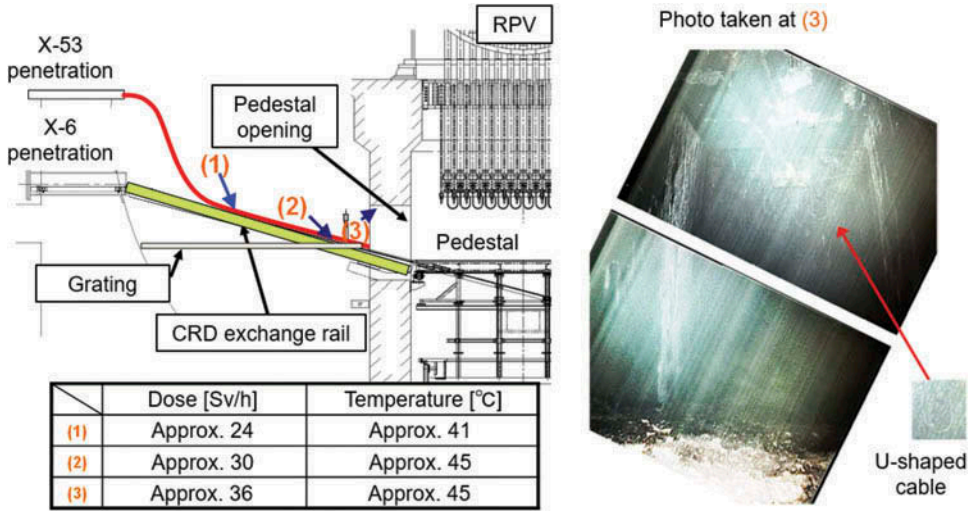

	Dose [Sv/h]	Temperature [°C]
(1)	Approx. 24	Approx. 41
(2)	Approx. 30	Approx. 45
(3)	Approx. 36	Approx. 45

Fig. 12. Interior of the Unit 2 pedestal (1/4) (Ref. 30).

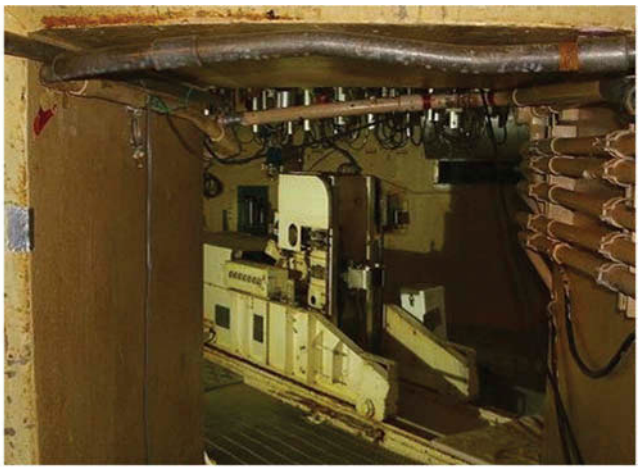

(a) Observing the inside of the platform from the pedestal opening

(b) Observing the bottom of the RPV

Fig. 13. Interior of the Unit 5 pedestal.[30]

PCV (Ref. 39). From this information and the muon measurement results in Estimation 11, we infer that several small openings may have been formed by the damage to the bottom of the RPV where the CRDMs are standing close together.

Thus, it is inferred that the holes in the RPV are focused around its center and are not very large. As water drops were falling on the entire surface of the pedestal floor, even though some parts had more water drops than other parts, several small openings may have been formed by the damage around the control rod drive (CRD) housing at the bottom of the RPV.

IV.C.5. Estimation 13 (Failure Site Outside of CRDs in the RPV Boundary)

The images captured in January 2018 during an inspection of the PCV interior using the guide pipe and the telescopic research device [Fig. 16 (Ref. 38)] show that the upper tie plate of the fuel assembly fell on the pedestal floor. Because it fell near the inner wall of the pedestal and the CRDs around the outer circumference remain, as shown in Estimation 12, the upper tie plate fell through the openings formed by the damage outside the area at the bottom of the RPV where the CRDs are standing close together.

Thus, because the upper tie plate has fallen on the outer circumference of the pedestal, the openings formed by the damage probably exist around the outer circumference of the RPV.

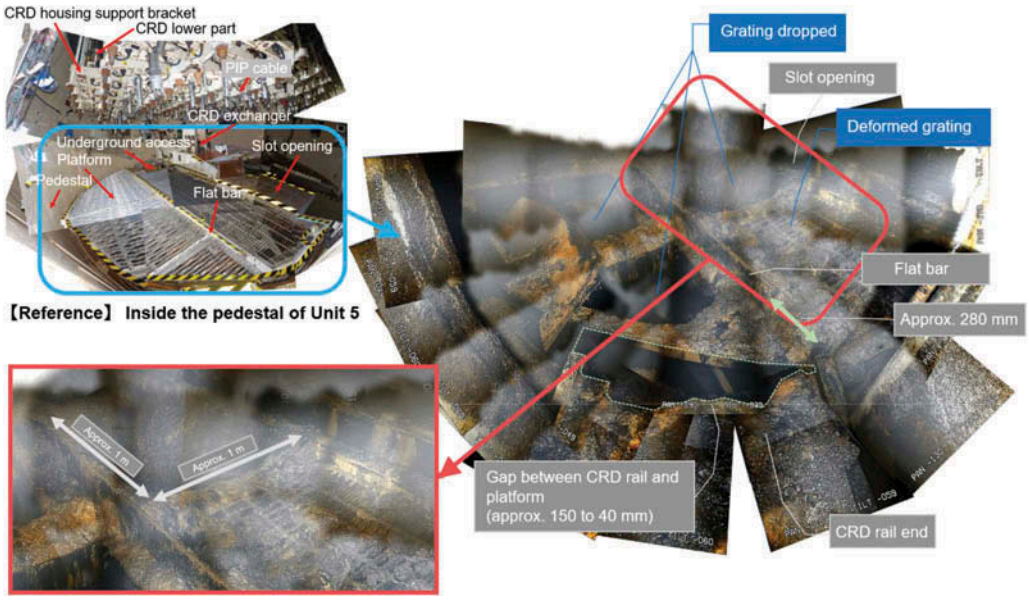

Fig. 14. Interior of the Unit 2 pedestal (2/4) (Ref. 40).

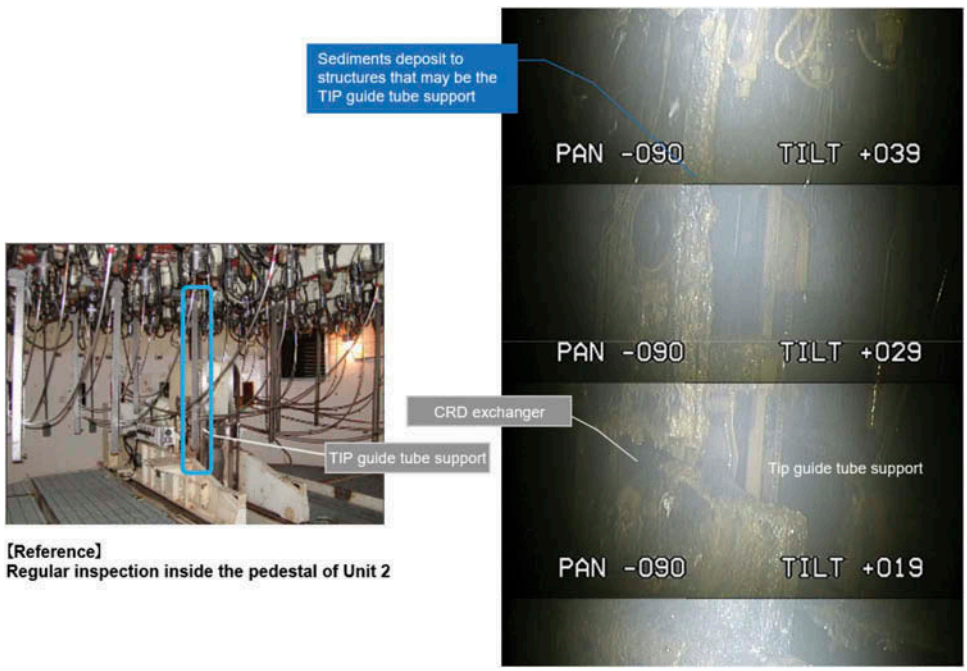

Fig. 15. Interior of the Unit 2 pedestal (3/4) (Ref. 40).

IV.C.6. Estimation 14 (Size of the RPV Failure Site Allowing the Tie Plate to Fall Down)

The images obtained during the inspection of the PCV interior using the guide pipe and the telescopic research device conducted in January 2018 [Fig. 16 (Ref. 38)] show that the upper tie plate of the fuel assembly fell on the pedestal floor. It may be inferred that there is a hole in the RPV that is at least large enough for the upper tie plate to fall through.

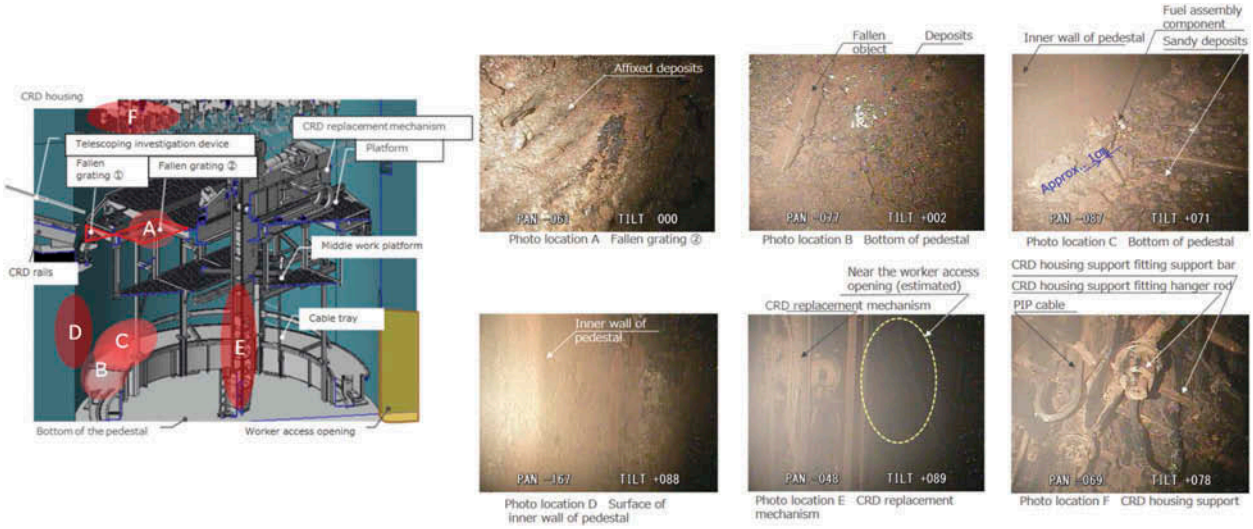

Fig. 16. Interior of the Unit 2 pedestal (4/4) (Ref. 38).

Thus, it is inferred that there is a hole at least large enough for the upper tie plate to fall through.

IV.C.7. Estimation 15 (Melting/Collapse of CRD/CRGT in the Periphery)

The results of the inspection of the PCV interior conducted in January 2018 demonstrate that the debris are clearly spread all over the pedestal and the height of accumulated debris is unevenly distributed. A relatively large amount of debris may have fallen on the spots at which the accumulated height is particularly high, and the debris may have spread from these spots to the rest of the pedestal. Because the accumulation of debris is concentrated around the periphery of the pedestal and the upper tie plate of the fuel assembly is located inside the pedestal, an opening at least large enough for the upper tie plate to fall through is formed in the outer circumference at the bottom of the RPV, which is located above the pedestal. From the results of the analysis of event transition at the slumping of core materials,[2] in-depth analysis of the accident progression of Units 2 and 3 using the MAAP code,[2] and the BWR core degradation behavior confirmation test using the simulated duel assembly,[2] we infer that the path through which the upper tie plate fell is formed by the melting and collapse of the CRGT and CRD around the outer circumference.

Thus, judging from the debris accumulated at the bottom of the RPV, we infer that parts of the CRGT and CRD of the outer circumference melted and/or collapsed.

IV.D. The RPV and Inside the Pedestal

IV.D.1. Estimation 16 (Solidified Debris on the Outer Surface of CRD)

The general estimation suggests that if the fuel debris leaked from the welded section of the CRD piping, which can explain the opening in the RPV, the fuel debris may have solidified and adhered to the exterior of the CRD piping outside the RPV.

Thus, some of the debris that fell out of the hole is estimated to adhere on the CRD.

IV.D.2. Estimation 17 (Fuel Debris/Molten Metal Ingression into CRD Housing)

The general estimation implies that when the CRGT and CRD housing of the lower part of the RPV was ablated by the fuel debris, the fuel debris may have entered the CRD piping. Detailed evaluation of debris behavior after failures of the lower head and its inside that simulated the situation where the fuel debris ablated the CRD housing from the outside showed that the melted CRD housing entered the piping before the fuel debris.[2] Moreover, because the CRD housing has small vertical thermal conductions and its shape prevents the release of heat, it gets easily ablated when it comes into contact with high-temperature fuel. When the melted fuel debris has a higher temperature, it is in the fluid state and can penetrate more deeply into the CRD piping. However, if the decay heat of the fuel debris that entered the piping is high, it can invade even more deeply as it melts the

CRD piping. On the other hand, if the fuel debris comes into contact with the water inside the CRD piping, its invasion is hindered. Furthermore, when the decay heat of the fuel debris per volume is smaller due to its metal content or emitting volatile radioactive nuclear FPs, thermal emission may have been limited because the capacity inside the CRD piping is small and some fuel debris had solidified inside the piping when reaching equilibrium with the heat released from the CRD housing. At Unit 2, the fuel was cooled for approximately 3 days thanks to the activation of the RCIC system. Therefore, the fuel debris had less decay heat than in other units as it moved to the lower plenum. Moreover, because alternate water injection was also being conducted, the fuel debris had more difficulty in entering the CRD piping than it did in other units.

Therefore, a small amount of fuel debris or melted metal may have entered the CRD housing after the damage to the CRGT and CRD housing occurred.

IV.D.3. Estimation 18 (Particulate Debris Formation)

When leakage from, for instance, the sealed pump mechanism of the PLR is considered, water may have started to accumulate on the floor where the bottom of the RPV was damaged, and the fuel debris fell to the floor inside the pedestal. In this case, particle-shaped debris may have formed when the falling high-temperature fuel debris encountered water.

Thus, particle-shaped debris was formed where there is accumulated water on the PCV floor.

IV.D.4. Estimation 19 (Particulate Debris Accumulation in the Stagnant Locations)

The general estimation infers that there is a possibility that particle-shaped debris has accumulated on the stagnant parts inside the pedestal, similar to the lower part of the RPV.

Thus, there is a possibility that when there is particle-shaped debris, it accumulates on stagnant parts.

IV.D.5. Estimation 20 (Spreading of Fuel Debris)

The footage obtained from the inspection of the PCV interior using the guide pipe and the telescopic research device conducted in January 2018 shows the spread of accumulation all over the bottom of the pedestal. This accumulation is assumed to contain the fuel debris.

Thus, it is inferred that accumulation containing fuel debris spreads all over the bottom of the pedestal.

IV.D.6. Estimation 21 (Relocation Path of Debris in the Vicinity of the Tie Plate)

The image obtained during the inspection of the PCV interior using the guide pipe and the telescopic research device conducted on January 2018 [Fig. 16 (Ref. 38)] demonstrates that the upper tie plate of the fuel assembly fell on the pedestal floor. If the fuel debris fell through the same hole the upper tie plate fell through, it may be inferred that the accumulation near the fallen upper tie plate is fuel debris.

Thus, it is inferred that the accumulation near the upper tie plate, which fell on the pedestal floor, is fuel debris that fell through the same hole in the RPV as the upper tie plate.

IV.D.7. Estimation 22 (Possible Metal-Rich Debris)

The image obtained during the inspection of the PCV interior using the guide pipe and the telescopic research device conducted in January 2018 [Fig. 16 (Ref. 38)] indicates that the upper tie plate of the fuel assembly fell on the pedestal floor. If the fuel debris fell through the same hole that the upper tie plate fell through, it may be inferred that the accumulation near the fallen upper tie plate is fuel debris. Moreover, during the inspection of the PCV interior conducted in January 2018, dose rate and temperature were measured. Figure 17 (Ref. 38) shows the measurement results. The measurement results did not indicate any significant change in either the dose or the temperature from the pedestal floor to the platform, and their numbers were relatively small (dose: 7 to 8 Gy/h; temperature: 21.0°C). Thus, it is inferred that the contribution to the dose or as a heat source from the fuel debris that fell on the pedestal floor was relatively small. There was no conspicuous damage to the lower structure of the pedestal, such as the cable tray, and the accumulation of fuel debris spreads all over the pedestal floor, though there are some local differences in the accumulation height. From these facts, it is inferred that the fuel debris was in a low-temperature state with a certain degree of fluidity when it fell. Moreover, from the fact that most of the fuel debris inside the pedestal had cooled down even though it was exposed, it is inferred that there is a possibility that the fuel debris accumulated on the pedestal is composed of a material comprising a high metal component and low melting point.

Thus, it is inferred that the fuel debris on the pedestal floor has relatively low dose and decay heat and may contain large amounts of metal because no changes in dose or temperature were detected between the pedestal

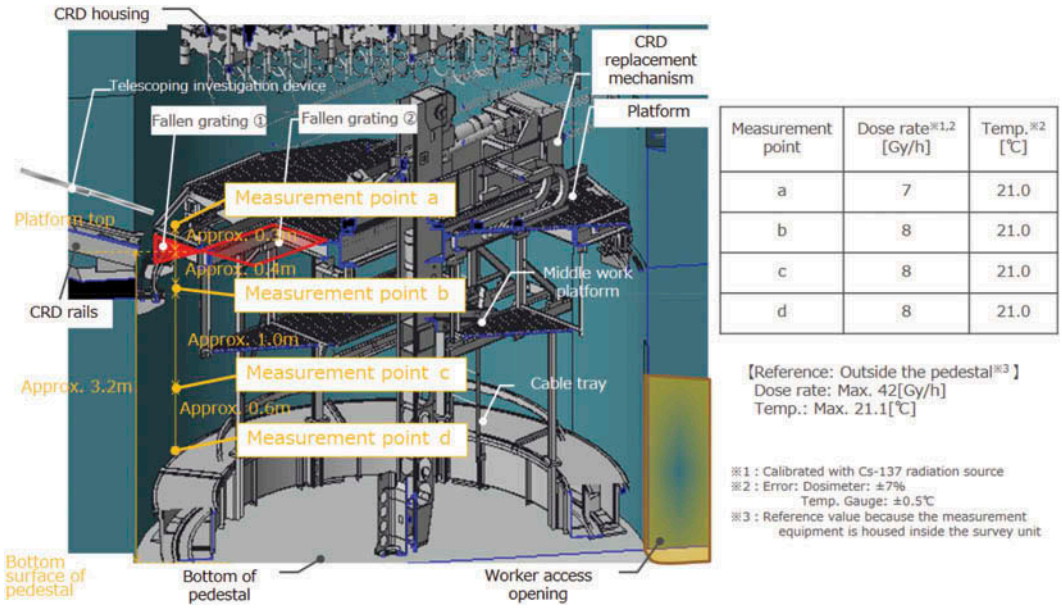

Fig. 17. Results of dose rate and temperature measurements inside the pedestal.[38]

floor and the platform and no conspicuous damage was observed to the lower structure of the pedestal.

IV.D.8. Estimation 23 (Debris Composition If MCCI Is Concerned)

The fuel debris that fell on the pedestal could have triggered molten core–concrete interaction (MCCI) and got mixed with the concrete. Note that the muon measurement results discussed in Estimation 11 indicate the possibility that a large amount of fuel debris accumulated in the lower plenum of the RPV. Thus, the amount of fuel debris that fell in the pedestal is probably quite small, and the spread of fuel debris within the pedestal is probably limited.

Thus, it is inferred that the fuel debris that resulted in the MCCI is mixed in with the concrete.

IV.D.9. Estimation 24 (MCCI is Not Significant: From PCV Boundary Integrity)

The inspection of the torus room interior conducted at Unit 2 showed no evidence of the damage to the containment shell, such as leakage from the sand cushion drain pipe, which was observed in Unit 1. As shown in Fig. 18 (Ref. 47), verification of the leakage from the area around the lower part of the suppression chamber (S/C) vent pipe using a quadruped walking robot was conducted in December 2012 and April 2013. These inspections were conducted at "①" the vent pipe sleeves, "②" the ends of the sand cushion drain pipes, and "③" the lower parts of the vent pipe bellows that cover the eight vent pipes as shown in Fig. 18 (Ref. 47), and no leakage was found [Fig. 19 (Ref. 47)]. Thus, it is inferred that even if the fuel debris that fell in the pedestal reacted with the concrete, it occurred within a limited area.

Thus, it is inferred that the MCCI was limited as there was no tendency for damage to the PCV shell (no leakage from the sand cushion drain pipe).

IV.D.10. Estimation 25 (MCCI Is Not Significant: From Structure Integrity Inside Pedestal)

The image obtained during the inspection of the PCV interior using the guide pipe and the telescopic research device conducted in January 2018 [Fig. 16 (Ref. 38)] indicates that the pedestal walls, the cable tray by the wall, and the pillar of the CRD exchange mechanism did not melt. Thus, it may be inferred that the temperature of the fuel debris was low when it fell and spread on the pedestal, and even if it reacted with the concrete, it affected only a limited area.

Thus, there is a possibility that the MCCI was limited because the pedestal walls, the cable tray, and the pillar of the CRD exchange mechanism did not melt.

IV.D.11. Estimation 26 (Most of Solidified Debris Without MCCI)

The video obtained during the inspection of the PCV interior conducted in January 2018 (Ref. 39) verifies the accumulation of fuel debris on the cable tray in the pedestal.

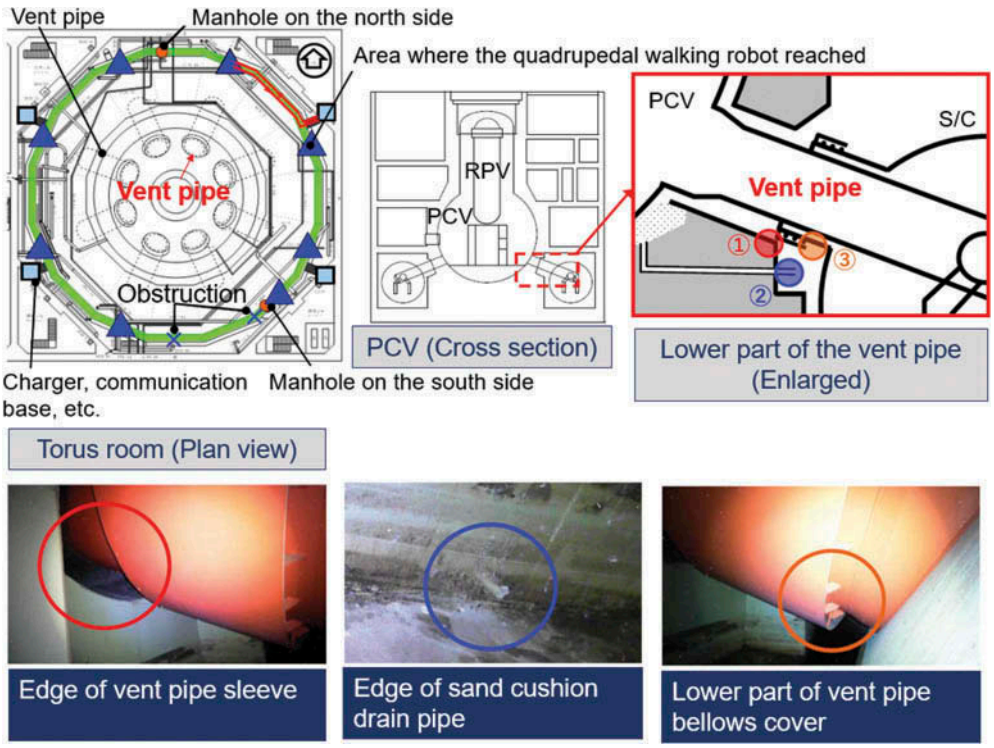

Fig. 18. Sections of the lower part of the vent pipe to be inspected.[47]

No.	Investigation date	Edge of vent pipe sleeve	Edge of sand cushion drain pipe	Lower part of vent pipe bellows cover
①	Dec. 11, 2012	X	X	X
②※2	Mar. 6, 2013	X	X	X
③※2	Mar. 5, 2013	X※1		X
④※2	Mar. 5, 2013	X※1		X
⑤※2	Mar. 13, 2013	X※1		X
⑥※2	Mar. 13, 2013	X※1		X
⑦※2	Mar. 14, 2013	X	X	X
⑧※2	Mar. 15, 2013	X	X	X

X : No leakage.
※1 : Although not confirmed directly, there is no flowing water on the lower concrete stage.
※2 : Sound data has also been acquired. No sound has been identified that may have leaked.

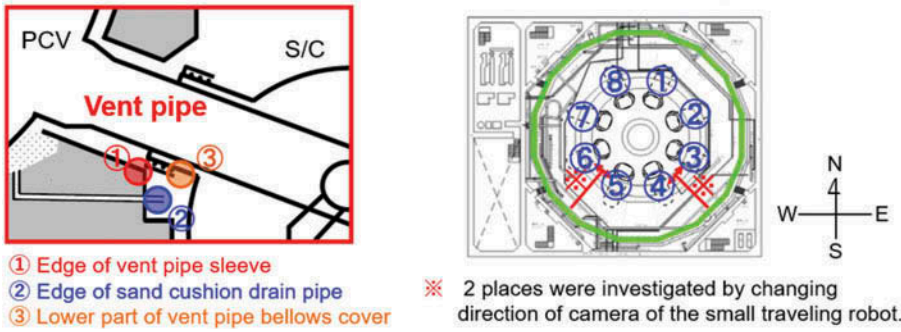

Fig. 19. Inspection results of the area around the lower part of the Unit 2 vent pipe.[47]

As the cable tray remained undamaged, there is a possibility that this accumulation has low heat generation density. It is necessary for the fuel debris that fell on the pedestal to increase the temperature of the concrete beyond its melting point to cause MCCI. However, as its decay heat may be inferred to be sufficiently low, attributed to the fact that the cable tray maintained its shape, there is a possibility that parts of the fuel debris that fell on the pedestal were cooled down at an early stage by the retained water of the pedestal and solidified without triggering significant MCCI.

Thus, there is a possibility that some of the fuel debris solidified without triggering significant MCCI.

V. CONCLUSION

We will continue to collect new information from on-site studies and will incorporate this information in future estimations of the debris distribution. Though some data may change because of the estimations reported above, we plan to continue research into the state of the reactors that experienced the accident at 1F. These estimations will contribute to the development of effective policies for removing fuel debris from the site.

Acknowledgments

The content of this material includes output of the Ministry of Economy, Trade and Industry subsidy for Project of Decommissioning and Contaminated Water Management (Upgrading for Identifying Comprehensive Conditions Inside the Reactor).

ORCID

Takuya Yamashita http://orcid.org/0000-0002-7340-9427

References

1. S. MIZOKAMI, "Estimation of Current Status Inside RPV and PCV at Fukushima Daiichi NPS," Tokyo Electric Power Company Holdings; https://ndf-forum.com/2nd/ref/d2_mizokami_en.pdf (current as of Dec. 5, 2019).
2. "Hairo/osensuitaisakujigyohihojokin (Sogoteki Na Ronaijyo-ukyouhaaku No Kodoka)," International Research Institute for Nuclear Decommissioning; http://irid.or.jp/_pdf/20170000_01.pdf (current as of Dec. 5, 2019) (in Japanese).
3. "Report on Measures Based on Temperature Rise in the Bottom Section Reactor Pressure Vessel of Reactor #2 at the Fukushima Daiichi Nuclear Power Station," Tokyo Electric Power Company; http://www.tepco.co.jp/en/press/corp-com/release/betu12_e/images/120216e5.pdf (current as of Dec. 5, 2019).
4. "1, 2GOUKI Torasushitsutairyusui Oyobi Taisekibutsu Bunsekikekka Nitsuite," Tokyo Electric Power Company; http://warp.da.ndl.go.jp/info:ndljp/pid/9516313/www.meti.go.jp/earthquake/nuclear/pdf/130828/130828_01gg.pdf (current as of Dec. 5, 2019) (in Japanese).
5. "Results of Additional Work in Soundness Inspection of Unit 2 TIP Guide Pipe," Tokyo Electric Power Company; http://www.tepco.co.jp/en/nu/fukushima-np/handouts/2013/images/handouts_130719_07-e.pdf (current as of Dec. 5, 2019).
6. "2GOUKI Tipannaikanfuchakubutsu No Kanikinzokubunsekikekka Nitsuite," Tokyo Electric Power Company; https://www.meti.go.jp/earthquake/nuclear/pdf/131128/131128_01m.pdf (current as of Dec. 5, 2019) (in Japanese).
7. "Fukushima Daiichi Genshiryoku Hatsudensho No Sample Bunseki Nitsuite," Tokyo Electric Power Company Holdings; http://www.tepco.co.jp/nu/fukushima-np/handouts/2017/images2/handouts_171030_07-j.pdf (current as of Dec. 5, 2019) (in Japanese).
8. "Locating Fuel Debris Inside the Unit 2 Reactor Using a Muon Measurement Technology at Fukushima Daiichi Nuclear Power Station," Tokyo Electric Power Company; http://www.tepco.co.jp/en/nu/fukushima-np/handouts/2016/images/handouts_160728_01-e.pdf (current as of Dec. 5, 2019).
9. "2GOUKI Pcv Naibu Saichousakekka Nitsuite," Tokyo Electric Power Company; http://warp.da.ndl.go.jp/info:ndljp/pid/11241027/www.meti.go.jp/earthquake/nuclear/pdf/130828/130828_01hh.pdf (current as of Dec. 5, 2019) (in Japanese).
10. "Fukushima Daiichi Genshiryoku Hatsudensho 1-3GOUKI No Roshin Sonshou Jyoukyo No Suitei Nitsuite," Tokyo Electric Power Company; http://www.tepco.co.jp/nu/fukushima-np/images/handouts_111130_09-j.pdf (current as of Dec. 5, 2019) (in Japanese).
11. "2GO Rpv Teibu Ondokei No Sonyusagyokekka Nitsuite," Tokyo Electric Power Company; http://warp.da.ndl.go.jp/info:ndljp/pid/10217941/www.meti.go.jp/earthquake/nuclear/pdf/150326/150326_01_3_01_02.pdf (current as of Dec. 5, 2019) (in Japanese).
12. "FUKUSHIMADAIICHI/1-3GOUKI Koremadeno Chusuiryo Henkoji No Ondokyodo Nitsuite," Tokyo Electric Power Company; http://warp.da.ndl.go.jp/info:ndljp/pid/11241027/www.meti.go.jp/earthquake/nuclear/pdf/140227/140227_02j.pdf (current as of Dec. 5, 2019) (in Japanese).
13. "Fukushima Daiiti Genshiryoku Hatsudensho 1-3 Gouki Genshiro Tyusuiryo Teigen Nitsuite," Tokyo Electric Power Company Holdings; http://www.tepco.co.jp/nu/

fukushima-np/handouts/2017/images1/handouts_170522_05-j.pdf (current as of Dec. 5, 2019) (in Japanese).

14. "1, 2GOUKI Genshiro Tyusui Line No Pe Kanka Kouji Nitomonau Fdw Kei Tandoku Tyusui No Eikyo Kakunin Shiken No Jittshi Jyoukyo Nitsuite," Tokyo Electric Power Company Holdings; http://www.meti.go.jp/earthquake/nuclear/decommissioning/committee/osensuitaisakuteam/2017/08/3-05-04.pdf (current as of Dec. 5, 2019) (in Japanese).
15. "2GOUKI Kyusuikei Tyusui Line Kaizou Ni Tomonau Roshin Spray Kei Tandoku Tyusui No Jittshi Jyoukyo Nitsuite," Tokyo Electric Power Company Holdings; http://www.tepco.co.jp/nu/fukushima-np/roadmap/2018/images1/d180426_10-j.pdf#page=3 (current as of Dec. 5, 2019) (in Japanese).
16. "Tateyanai No Kukan Senryouritsu Nitsuite," Tokyo Electric Power Company; http://www.tepco.co.jp/nu/fukushima-np/f1/surveymap/images/f1-sv3-20140327-j.pdf (current as of Dec. 5, 2019) (in Japanese).
17. "2GOUKI X-6PENE Shuhen Josenjisshijyoukyou Nitsuite (Keikahokoku)," Tokyo Electric Power Company; http://warp.da.ndl.go.jp/info:ndljp/pid/9552510/www.meti.go.jp/earthquake/nuclear/decommissioning/committee/osensuitaisakuteam/2015/pdf/1126_3_3b.pdf (current as of Dec. 5, 2019) (in Japanese).
18. "2GOUKI Pcv Naibu Chosa Ni Muketeno X-6 Pene Mawari Jyosen Nitsuite," Tokyo Electric Power Company; http://www.meti.go.jp/earthquake/nuclear/decommissioning/committee/osensuitaisakuteam/2016/pdf/0331_3_3b.pdf (current as of Dec. 5, 2019) (in Japanese).
19. "Survey Results of TIP Room in Ground-Floor at Reactor Building, Unit 2 at Fukushima Daiichi Nuclear Power Station," Tokyo Electric Power Company; http://www.tepco.co.jp/en/nu/fukushima-np/images/handouts_120322_01-e.pdf (current as of Dec. 5, 2019).
20. "Fukushima Daiichi Genshiryoku Hatsudensho 2GOUKI Genshiro Tateyanai Tyousa Kettuka (3kai-5kai)," Tokyo Electric Power Company; http://www.tepco.co.jp/nu/fukushima-np/images/handouts_120614_02-j.pdf (current as of Dec. 5, 2019) (in Japanese).
21. "Fukushimadaiichigenshiryokuhatsudensho Nigouki Genshirotateyanai Tyousa Kettuka (3kai-5kai) (Heisei24nen6gatsu13nichijisshi)," Tokyo Electric Power Company; http://www.tepco.co.jp/nu/fukushima-np/images/handouts_120614_02-j.pdf (current as of Dec. 5, 2019) (in Japanese).
22. "Unit 2 Primary Containment Vessel Investigation at Fukushima Daiichi Nuclear Power Station (Addendum Report with Image Analysis)," Tokyo Electric Power Company Holdings; http://photo.tepco.co.jp/en/date/2017/201703-e/170330-01e.html (current as of Dec. 5, 2019).
23. "2GOUKI Genshiro Kakunouyouki Naibu Tyousa Nitsuite–Taisekibutsu Jyoukyo Sagyou No Jittshi," Tokyo Electric Power Company Holdings; http://www.tepco.co.jp/nu/fukushima-np/handouts/2017/images1/handouts_170206_05-j.pdf (current as of Dec. 5, 2019) (in Japanese).
24. "2GOUKI Genshiro Kakunou Youki Naibu Tyousa Oyobi Nenryou Deburi Toridashi Ni Muketa Taiou Jyoukyou," Tokyo Electric Power Company Holdings; http://www.tepco.co.jp/nu/fukushima-np/roadmap/2018/images1/d180531_08-j.pdf#page=3 (current as of Dec. 5, 2019) (in Japanese).
25. "2GOUKI Rpv Daitaiondokeisetchi Nimuketa Haikannai Mizunuki Hoho No Kentojyoukyou Nitsuite," Tokyo Electric Power Company; http://warp.da.ndl.go.jp/info:ndljp/pid/11241027/www.meti.go.jp/earthquake/nuclear/pdf/120827/120827_01k.pdf (current as of Dec. 5, 2019) (in Japanese).
26. "2GO Rpv Teibuondokei No Sonyu Sagyo Kettuka Nitsuite," Tokyo Electric Power Company; http://warp.da.ndl.go.jp/info:ndljp/pid/10217941/www.meti.go.jp/earthquake/nuclear/pdf/150326/150326_01_3_01_02.pdf (current as of Dec. 5, 2019) (in Japanese).
27. "Jikoshintenkaiseki Oyobi Jikkidetato Niyoru Ronai Jyoukyouu Haakunokodoka," International Research Institute for Nuclear Decommissioning; http://irid.or.jp/_pdf/201509to10_06.pdf?v=3 (current as of Dec. 5, 2019) (in Japanese).
28. "2GOUKI Genshirokakunoyoki Naibu Tyousa (2kaime) Nitsuite," Tokyo Electric Power Company; http://warp.da.ndl.go.jp/info:ndljp/pid/11241027/www.meti.go.jp/earthquake/nuclear/pdf/120328_02g.pdf (current as of Dec. 5, 2019) (in Japanese).
29. "Fukushimadaiichigenshiryokuhatsudensho 1/2GOUKI Haikito Tenke Kettuka Nitsuite," Tokyo Electric Power Company; http://warp.da.ndl.go.jp/info:ndljp/pid/11241027/www.meti.go.jp/earthquake/nuclear/decommissioning/committee/osensuitaisakuteam/2015/pdf/1029_4_3a.pdf (current as of Dec. 5, 2019) (in Japanese).
30. "Roshin/kakunoyokinai No Jotaisuitei Ni Kanrensuru Chosajyoukyou (Tempushiryo 4)," Tokyo Electric Power Company; http://www.tepco.co.jp/cc/press/betu15_j/images/151217j0109.pdf (current as of Dec. 5, 2019) (in Japanese).
31. "Result of the Second Investigation Inside of Primary Containment Vessels, Unit 2, Fukushima Daiichi Nuclear Power Plant," Tokyo Electric Power Company; http://www.tepco.co.jp/en/nu/fukushima-np/images/handouts_120326_07-e.pdf (current as of Dec. 5, 2019).
32. "2GOUKI Pcvnai Josetsukanshikeiki No Setchi Oyobi Tairyusui Saishu Nitsuite," Tokyo Electric Power Company; http://warp.da.ndl.go.jp/info:ndljp/pid/11241027/www.meti.go.jp/earthquake/nuclear/pdf/130828/130828_01h.pdf (current as of Dec. 5, 2019) (in Japanese).
33. "Fukushima Daiichi Nuclear Power Station Unit 2 Parameters of Water Level and Pressure," Tokyo Electric Power Company Holdings; http://www.tepco.co.jp/en/nu/

fukushima-np/plant-data/f1_8_Parameter_data_20110717.pdf (current as of Dec. 5, 2019).

34. "2GOUKI No 15NICHI No Cams Sokuteichi No Kyujosho Nitsuite (Tempushiryo 2-10)," Tokyo Electric Power Company; http://www.tepco.co.jp/cc/press/betu15_j/images/151217j0129.pdf (current as of Dec. 5, 2019) (in Japanese).

35. "Internal Exploration of the Unit 2 Primary Containment Vessel (PCV)—Reevaluation of Dose Rate Estimate," Tokyo Electric Power Company Holdings; http://www.tepco.co.jp/en/nu/fukushima-np/handouts/2017/images/handouts_170727_03-e.pdf (current as of Dec. 5, 2019).

36. "Fukushima Daiichi Genshiryoku Hatsudenso 2GOUKI Genshiro Kakunouyoukinai Kanshikeiki Saisetti Sagyou Kettuka," Tokyo Electric Power Company; http://www.tepco.co.jp/nu/fukushima-np/handouts/2014/images/handouts_140609_05-j.pdf (current as of Dec. 5, 2019) (in Japanese).

37. "The 5th Progress Report on the Investigation and Examination of Unconfirmed and Unresolved Issues on the Development Mechanism of the Fukushima Daiichi Nuclear Accident," Tokyo Electric Power Company Holdings; https://www4.tepco.co.jp/en/decommision/accident/images/171225e0101.pdf (current as of Dec. 5, 2019).

38. "Fukushima Daiichi Nuclear Power Station Unit 2 Primary Containment Vessel Internal Investigation Results," Tokyo Electric Power Company Holdings; http://www.tepco.co.jp/en/nu/fukushima-np/handouts/2018/images/handouts_180201_01-e.pdf (current as of Dec. 5, 2019).

39. "Progress of Unit 2 PCV Internal Investigation (Preliminary Report of January 19 Investigation)," Tokyo Electric Power Company Holdings; http://tepco.webcdn.stream.ne.jp/www11/tepco/download/180122_01j.zip (current as of Dec. 5, 2019).

40. "2GOUKI Genshiro Kakunouyouki Naibu Tyousa Nitsuite," Tokyo Electric Power Company Holdings; http://www.tepco.co.jp/nu/fukushima-np/roadmap/2017/images1/d170223_08-j.pdf (current as of Dec. 5, 2019) (in Japanese).

41. "Pre-Investigation Results of the Area Inside the Pedestal for the Unit 2 Primary Containment Vessel Investigation at Fukushima Daiichi Nuclear Power Station (Examination Results of Digital Images)," Tokyo Electric Power Company Holdings; http://www.tepco.co.jp/en/nu/fukushima-np/handouts/2017/images/handouts_170202_01-e.pdf (current as of Dec. 5, 2019).

42. "Unit 2 Primary Containment Vessel Internal Investigation," Tokyo Electric Power Company Holdings; http://www.tepco.co.jp/en/nu/fukushima-np/handouts/2017/images/handouts_171130_01-e.pdf (current as of Dec. 5, 2019).

43. "2gouki S/C nai Suii Sokuteikekka," Tokyo Electric Power Company; https://www.meti.go.jp/earthquake/nuclear/pdf/140130/140130_01kk.pdf (current as of Dec. 5, 2019) (in Japanese).

44. "2GOUKI No Atsuryokuyokuseishitsu(s/c) No Suiihenka to Ondohenka Nitsuite," Tokyo Electric Power Company Holdings; http://www.tepco.co.jp/cc/press/betu15_j/images/151217j0132.pdf (current as of Dec. 5, 2019) (in Japanese).

45. "TATEYATAIRYUSUISHORINOSHINCHOKUJYOUKY-"TATEYATAIRYUSUISHORINOSHINCHOKUJYOUKY-OUNITSUITE," Tokyo Electric Power Company Holdings; http://www.nsr.go.jp/data/000264774.pdf#page=20 (current as of Dec. 5, 2019) (in Japanese).

46. "2GOUKI Torus Shitsu Tyousa Kettuka," Tokyo Electric Power Company; http://www.tepco.co.jp/nu/fukushima-np/roadmap/images/d130426_05-j.pdf (current as of Dec. 5, 2019) (in Japanese).

47. "2GOUKI Bentokan Kabushuhen Chosakekka Nitsuit," Tokyo Electric Power Company; https://www4.tepco.co.jp/decommision/principles/technology/robot/robot_under/pdf/quadruped_w_robot_01.pdf (current as of Dec. 5, 2019) (in Japanese).

48. "Examination into the Reactor Pressure Increase After Forced Depressurization at Unit-2, Using a Thermal-Hydraulic Code (Attachment 2-9)," Tokyo Electric Power Company; https://www4.tepco.co.jp/en/press/corp-com/release/betu17_e/images/171225e0227.pdf (current as of Dec. 5, 2019).

49. "Tokyodenryoku Fukushimadaiichigenshiryokuhatsudensho 1-3GOUKI No Roshinsonshojyoukyou No Suitei Nitsuite," Tokyo Electric Power Company; http://www.tepco.co.jp/nu/fukushima-np/images/handouts_111130_07-j.pdf (current as of Dec. 5, 2019) (in Japanese).

50. "Fukushimadaiichigenshiryokuhatsudensho 2GOUKI Genshiroatsuryokuyokiteibu Niokeru Ondojosho Wo Fumaeta Taio Ni Kakawaru Hokoku Nitsuite," Tokyo Electric Power Company; http://www.tepco.co.jp/cc/press/betu12_j/images/120216a.pdf (current as of Dec. 5, 2019) (in Japanese).

51. T. YAMASHITA et al., "The CMMR Program; BWR Core Degradation in the CMMR-1 and the CMMR-2 Tests," *Proc. 12th Int. Conf. Croatian Nuclear Society—Nuclear Option for CO_2 Free Energy Generation*, Zadar, Croatia, 2018, p. 15 (2018).

52. T. YAMASHITA et al., "The CMMR Program: BWR Core Degradation in the CMMR-3 Test," *Proc. Int. Conf. Dismantling Challenges—Industrial Reality, Prospects and Feedback Experience (DEM 2018)*, Avignon, France, 2018, p. 11 (2018).

53. T. YAMASHITA and I. SATO, "The CMMR Program—BWR Core Degradation in the CMMR-4 Test," *Proc. 9th European Review Mtg. Severe Accident Research (ERMSAR 2019)*, Prague, Czech Republic, 2019, p. 13 (2019).